

## Electronic Structure of Chainlike Polysilane

Kyozauro Takeda,\* Hiroyuki Teramae, and Nobuo Matsumoto

Contribution from the NTT Electrical Communications Laboratories, Musashino-shi, Tokyo 180, Japan. Received September 16, 1985

**Abstract:** Energy band structures are calculated for  $-(\text{SiXY})_n$  polysilane, model compounds in which X and Y are H, Me, Et, Pr, and Ph (phenyl) substituents. Polysilane has a directly allowed type band structure, and a  $\sigma$ - $\sigma^*$  interband optical transition is allowed. Band-edge states are formed mainly of skeleton Si AOs (atomic orbitals), which results in a skeleton band gap. This skeleton band gap tends to be reduced when larger alkyl groups are substituted for side chains. The  $\sigma$  and  $\sigma^*$  band-edge states are well delocalized on the skeleton axis. Polysilane with Ph side chains [poly(arylsilane)] exhibits a characteristic band-edge structure due to  $\sigma$ - $\pi$  mixing between the Si skeleton and Ph side chains. This interaction removes the doubly degenerated Ph  $\pi$ -HOMO states. One state is mixed with the skeleton  $\sigma$ -valence band state and delocalized along the skeleton axis. The other remains strongly localized in the individual Ph side chains. However, no  $\sigma^*$ - $\pi^*$  mixing occurs at the conduction band edge, and no change is seen in the conduction band structure. This results in the intrusion of unoccupied localized states in the skeleton band gap.

Recently, much attention has been paid to the semiconducting properties of polysilanes having a Si skeleton. Studies have dealt with properties such as the wide optical band gap,<sup>1,2</sup> photoluminescence,<sup>3</sup> photoconduction,<sup>4</sup> and doping effects.<sup>5</sup> An interpretation of these phenomena requires an understanding of the underlying electronic structure, especially the band-edge electronic structure including the conduction band. However, little theoretical work has been done on the electronic structure of poly(organosilane), compared with polymers having a C skeleton.<sup>6</sup> Theoretical studies have been carried out only for poly(hydrosilane), which is the simplest form of this material with H side chains.<sup>7,8</sup>

In this paper, the electronic structure of poly(organosilane) including its conduction band is investigated systematically by substituting several side chains. Three alkyl (R = Me, Et, and Pr) and phenyl (Ph) groups are used as the side-chain substituents. These are typical saturated and unsaturated substituents, respectively. These four substituent groups were combined in various ways to produce 10 polysilane model compounds (7 poly(alkylsilane) and 3 poly(arylsilane) compounds). The theoretical results are discussed on the basis of photoabsorption spectra determined experimentally.

## Theory

A semiempirical band calculation method known to describe the band-edge structure including the conduction band was used in order to systematically investigate the polysilane band-edge electronic structure. The method is based on Slater and Koster's (SK) LCAO approach,<sup>9</sup> because of the covalency in polysilane. In the LCAO method, the eigenfunctions  $\phi_i^\alpha$  of the bound states of free atoms are used as the basis, and the wave function for an electron in solids can be expressed in terms of Bloch sums as eq 1. The sum over eigenfunctions should be taken both over atomic

$$\bar{\Psi}_j(\vec{k}, \vec{r}) = \sum_{\vec{R}_n} e^{i\vec{k}\cdot\vec{R}_n} \sum_{l\alpha} a_{l\alpha} \bar{\phi}_l^\alpha(\vec{r}-\vec{R}_n) \quad (1)$$

species ( $\alpha$ ) involved in the unit cell and over quantum states ( $l$ ) of the corresponding AO. It is known, however, that the valence orbital approximation provides a good approximation for the Si and C elements in polysilane. Then, the valence eigenfunctions of Si-3s, Si-3p<sub>x</sub>, Si-3p<sub>y</sub>, Si-3p<sub>z</sub>, C-2s, C-2p<sub>x</sub>, C-2p<sub>y</sub>, C-2p<sub>z</sub>, and H-1s AOs are employed as the basis for  $l$  summation in this calculation. According to the conventional variation technique, the following familiar secular equation can be obtained.

$$|\epsilon_i \sum e^{i\vec{k}\cdot\vec{R}_n} \langle \phi_{j(\vec{r}-\vec{R}_n)} | \phi_{i(\vec{r})} \rangle + \sum e^{i\vec{k}\cdot\vec{R}_n} \langle \phi_{j(\vec{r}-\vec{R}_n)} | \hat{H} | \phi_{i(\vec{r})} \rangle - E \sum e^{i\vec{k}\cdot\vec{R}_n} \langle \phi_{j(\vec{r}-\vec{R}_n)} | \phi_{i(\vec{r})} \rangle | = 0 \quad (2)$$

One of the major problems in carrying out the SK LCAO approach is the determination of interatomic matrix elements  $\langle \phi_j | \hat{H} | \phi_i \rangle$  (LCAO parameters). In the empirical approach, these elements are treated as disposable constants, rather than computing the various integrals analytically, and are chosen so as to fit the results obtained experimentally (or by some other theoretical technique). A shortcoming of this empirical LCAO approach is the occasional need to determine those LCAO parameters for individual materials. This becomes disadvantageous for the systematic investigation of polysilane electronic structure.

Harrison<sup>10</sup> and Froyen et al.<sup>11</sup> found that LCAO bands provide a good description of the true bands and also resemble the free-electron bands. They succeeded in representing the LCAO parameters in terms of free-electron band parameters by fitting the LCAO bands to the free-electron bands at several points of highest symmetry  $\Gamma$  and X, taking into account the band-gap correction. In their formation, the interatomic matrix elements can be expressed as eq 3, where  $\kappa$  represents  $\sigma$ - or  $\pi$ -bonding and  $d$  means

$$\langle \phi_j | \hat{H} | \phi_i \rangle = E_{ij\kappa(uvw)} = \zeta_{l'l'm} \frac{\hbar^2}{md^2} \quad (3)$$

interatomic distance. The subscripts  $u$ ,  $v$ , and  $w$  are direction cosines for positional vector  $\vec{R}_n$ . The symbols  $l$  and  $l'$  on the right-hand side indicate the azimuthal quantum number for individual atomic orbitals labeled by s ( $l = 0$ ) or p ( $l = 1$ ), and  $m$  is the magnetic quantum number labeled by  $\sigma$  ( $m = 0$ ) or  $\pi$  ( $m = 1$ ). The parameter  $\zeta_{l'l'm}$  is the Harrison coefficient. For typical atomic configurations such as a diamond, a simple cube, and *bcc* and *fcc* crystal structures, Harrison and Froyen et al. obtained  $\zeta_{l'l'm}$  values which differed only slightly depending on the atomic

(1) (a) Wolford, D. J.; Scott, B. A.; Reimer, J. A.; Bradleg, J. A. *Physica B&C (Amsterdam)* **1983**, *117B*, 118B, 920. (b) Wolford, D. J.; Reimer, J. A.; Scott, R. A. *Appl. Phys. Lett.* **1983**, *42*, 369.

(2) Furukawa, S.; Matsumoto, N. *Solid State Commun.* **1983**, *48*, 539.

(3) Kagawa, T.; Fujino, M.; Takeda, K.; Matsumoto, N. *Solid State Commun.* **1986**, *57*, 635.

(4) Fujino, M., private communication.

(5) West, R.; David, L. D.; Djurovich, P. I.; Stearley, K. L.; Srinivasan, K. S. V.; Yu, H. *J. Am. Chem. Soc.* **1981**, *103*, 7352.

(6) (a) Whangbo, M. H.; Hoffmann, R.; Woodward, R. B. *Proc. R. Soc. London, A* **1979**, *366*, 23. (b) Duke, C. B.; Ford, W. K. *Int. J. Quantum Chem., Quantum Chem. Symp.* **1983**, *17*, 597.

(7) Teramae, H.; Yamabe, T.; Imamura, A. *Theor. Chim. Acta.* **1983**, *64*, 1.

(8) Weidman, R. S.; Bedford, K. L.; Kunz, A. B. *Solid State Commun.* **1981**, *39*, 917.

(9) Slater, J. C.; Koster, G. F. *Phys. Rev.* **1954**, *94*, 1498.

(10) Harrison, W. A. *Electronic Structure and the Properties of Solids*; Freeman: San Francisco, 1979.

(11) Froyen, S.; Harrison, W. A. *Phys. Rev. B: Condens. Matter* **1979**, *20*, 2420.

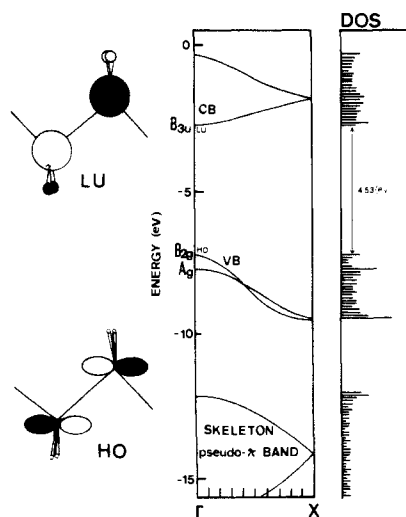


**Figure 1.** Energy band structure of  $(\text{SiH}_2)_n$  in ideal chain. Highest occupied (HO) and lowest unoccupied (LU) orbitals are sketched in terms of LCAO coefficients. Orbital lobes are drawn proportional to AO coefficients. Only orbitals with coefficients  $> 0.200$  are shown. Right side: energy dependence of density of states (DOS).

configuration. Therefore, they chose to introduce a universal value for  $\zeta_{ll'm}$  by adjusting the corresponding values for several kinds of crystal structures. The consistency of applying this universal value to polysilane has already been discussed by the authors in a previous work.<sup>12</sup> With the Harrison-Froyen method, the LCAO parameter can be estimated from as little information as a knowledge of corresponding bond lengths. Under these circumstances, the values are changed from a disposable constant to an individually unique value. Thus combining the SK LCAO approach and Harrison's method results in a semiempirical band calculation method based on the free-electron band theory and also makes the systematic investigation of polysilane electronic structure possible. In the present band calculation, non-nearest-neighbor interactions are also taken into account.

The symbol  $\epsilon_i$  in eq 2 represents the energy eigenvalues for the atomic Hamiltonian. In chainlike polymers, however, these values tend to differ from those for an isolated atomic Hamiltonian due to the formation of the chain structure. Using Herman and Skillman's<sup>13</sup> (HS)  $\epsilon_i$  values directly results in an overestimated ionized potential (IP). Therefore, the HS  $\epsilon_i$  values for Si, C, and H must be corrected to produce reasonable IP values<sup>14</sup> or consistent band structures. First, we fitted our calculated benzene IP value to an experimental value.<sup>15</sup> This fitting procedure corrects the  $\epsilon_i$  values for C-2s, C-2p, and H-1s.  $\epsilon_i$  values for Si-3s, Si-3p, C-2s, C-2p, and H-1s are then refined so as to yield consistent IP values estimated from  $-(\text{SiMe}_2)_n$  oligomer and their UPS spectra.<sup>16</sup> The resulting adjusted HS  $\epsilon_i$  values are  $\epsilon_{3s}(\text{Si}) = 8.0$ ,  $\epsilon_{3p}(\text{Si}) = -2.0$ ,  $\epsilon_{2s}(\text{C}) = -11.5$ ,  $\epsilon_{2p}(\text{C}) = -8.0$ , and  $\epsilon_{1s}(\text{H}) = -12.0$  eV.

It is necessary to determine the skeleton atomic configuration to calculate the polymer electronic structure. It is, however, not clear whether the Si skeleton is a trans-type planar zigzag or a helical coil, in spite of the observation of IR spectra originating from the poly(hydrosilane) chain structure.<sup>17</sup> Also, there is not enough information to determine polysilane atomic geometry. The

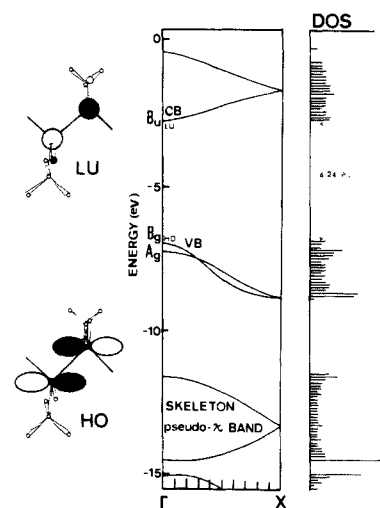


**Figure 2.** Energy band structure of  $(\text{SiHMe})_n$  model compound.

ab initio MO calculation is not yet capable of describing the stable form.<sup>18</sup> Therefore, the discussion in this work is based on the assumption that the skeleton is a trans-planar type. Alkyl side chains (R) are also assumed to form an all-trans-type geometry. The resulting poly(organosilane), having the same side chains,  $-(\text{SiX}_2)_n$ , has a  $D_{2h}$  symmetry. For poly(organosilane) having the different side chains,  $-(\text{SiXY})_n$ , X and Y substituents are alternatively substituted to form a  $C_{2h}$  symmetry. For the systematic investigation, bond lengths are quoted from Phillips-rationalized radii<sup>19</sup> ( $d_{\text{Si}} = 1.17$ ,  $d_{\text{C}} = 0.77$ , and  $d_{\text{H}} = 0.37$  Å).

## Results and Discussion

### Polysilane Having Small Alkyl Side Chains: Poly(alkylsilane).

The simplest form of polysilane is a poly(dihydrosilane),  $-(\text{SiH}_2)_n$ . The resulting energy structure of  $-(\text{SiH}_2)_n$  is shown in Figure 1. Band-edge states with different parities exist at the  $\Gamma$ -point.  $-(\text{SiH}_2)_n$  results in a directly allowed type band structure with a 4.53-eV band gap. Both band-edge states are composed mainly of skeleton Si atomic orbitals (AOs); the valence band (VB) edge is the bonding state between the skeleton Si-3p<sub>x</sub> (along the skeleton axis) AOs, and the conduction band (CB) edge is the antibonding state between the skeleton Si-3s AOs. This means that both of the band-edge states are well delocalized along the Si skeleton axis and have k dispersion. The band-edge states of  $-(\text{SiH}_2)_n$  can be assigned at the  $\Gamma$ -point as follows: the VB top state has B<sub>2g</sub> symmetry and the CB bottom state has B<sub>3u</sub> symmetry. An optical interaction occurs between these states when polarized light is injected within the skeleton plane. A "band-to-band" optical transition ( $\sigma$ - $\sigma^*$ ) results. The resulting skeleton pseudo- $\pi$ - and pseudo- $\pi^*$ -bands, which are formed by the  $\pi$ - $\pi$  coupling between neighboring skeleton Si AO components (3p<sub>z</sub>; vertical-to-skeleton plane), exist far from the Fermi level and are buried deep in the  $\sigma$ -VB and  $\sigma^*$ -CB band, respectively.

Poly(hydromethylsilane),  $-(\text{SiHMe})_n$ , is produced by substituting a Me group in the  $-(\text{SiH}_2)_n$  side chain. Figure 2 shows the calculated energy structure of  $-(\text{SiHMe})_n$ . This poly(organosilane) also has a directly allowed type band structure, and the band-edge states are similar to the LCAO pattern symmetry formed by  $-(\text{SiH}_2)_n$ ; the VB edge is the bonding state between skeleton Si-3p<sub>x</sub> AOs with B<sub>g</sub> symmetry, and the CB edge is the antibonding state between skeleton Si-3s AOs with B<sub>u</sub> symmetry. This side-chain substitution reduces the corresponding skeleton band gap to 4.24 eV. The Si-3p<sub>z</sub> AO contribution in the Si skeleton  $\sigma$ -band is augmented. This means that the skeleton  $\pi$ -like bonding characteristics (in other words, the degree of Si-3p<sub>z</sub> AO mixing) in the  $\sigma$ -skeleton band of  $-(\text{SiHMe})_n$  tends to be enhanced more than that of  $-(\text{SiH}_2)_n$ . It should be also noted that

(18) Teramae, H., private communication.

(19) Phillips, J. C. *Bonds and Bands in Semiconductors*; Academic: New York, 1973; p 22.

(12) Takeda, K.; Matsumoto, N.; Fukuchi, M. *Phys. Rev. B: Condens. Matter* **1984**, *30*, 5871.

(13) Herman, F.; Skillman, S. *Atomic Structure Calculation*; Prentice Hall: Englewood Cliffs, NJ, 1963.

(14) Pitt, C. G.; Bock, H. *J. Chem. Soc., Chem. Commun.* **1972**, 28.

(15) Kimura, K.; Katsumata, S.; Achiba, Y.; Yamazaki, T.; Iwata, S. *Handbook of HeI Photoelectron Spectra of Fundamental Organic Molecules*; Halsted: New York, 1981.

(16) (a) Bock, H.; Ensslin, W. *Angew. Chem., Int. Ed. Engl.* **1971**, *10*, 404. (b) Seki, K., private communication. (c) Bock, H.; Ensslin, W.; Feher, F.; Freund, R. *J. Am. Chem. Soc.* **1976**, *98*, 668. (d) Ensslin, W.; Bergmann, H.; Elbel, S. *J. Chem. Soc., Faraday Trans. 2* **1975**, *71*, 913.

(17) Furukawa, S.; Matsumoto, N.; Toriyama, T.; Yabumoto, N. *J. Appl. Phys.* **1985**, *58*, 4658.

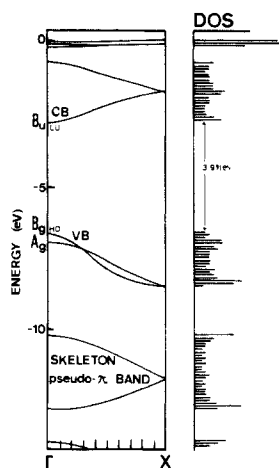


Figure 3. Energy band structure of  $(\text{SiMePr})_n$  model compound.

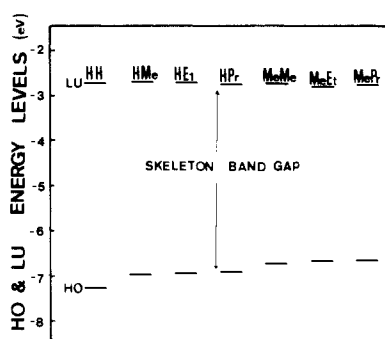


Figure 4. Skeleton band gap of poly(alkylsilane). HO, highest occupied level in valence band; LU, lowest unoccupied level in conduction band. Symbols H, Me, Et, and Pr indicate hydrogen atom, methyl, ethyl, and propyl substitution groups, respectively.

the Me group electron donation approaches the skeleton pseudo- $\pi$ - and pseudo- $\pi^*$ -bands toward the VB and CB edges, respectively. The  $\pi$ -bonding strength in the pseudo- $\pi$ -band is, however, weakened due to the other Si AOs mixing. This is confirmed by the pseudo- $\pi$ -bandwidth narrowing. The electronic states localized in the methyl side chains are found deep in the VB (-21 eV) and CB (4 eV). The overlap between neighboring Me groups through H atoms is small, since the Me group and H atom side chains are assumed to be alternatively substituted in the unit cell. This is the reason these localized states show poor dispersion.

Figure 3 shows the calculated energy band structure of poly(methylpropylsilane),  $(\text{SiMePr})_n$ . In spite of larger side chains, the reduction of the skeleton band gap is not significant ( $E_g = 3.91$  eV). The reason is that the band-edge states are determined mainly by skeleton Si AO contributions and that the side-chain substitution exerts little effect on the polysilane skeleton band gap (Figure 4). The resulting band-edge states in  $(\text{SiMePr})_n$  are analogous to the symmetrical LCAO patterns in  $(\text{SiHMe})_n$ . This produces a similar  $\sigma$ - $\sigma^*$  skeleton band optical transition. The shift of the skeleton pseudo- $\pi$ - and pseudo- $\pi^*$ -bands toward the band edges is found (Figure 5). The  $\pi$ -like bonding property in the poly(organosilane) skeleton  $\sigma$ -band also tends to be enhanced when side chains are substituted by larger alkyl groups. However, the higher state of the skeleton pseudo- $\pi$ -bands is never raised beyond the original  $\sigma$ -HO VB state because of the single  $\sigma$ -bond formation of the polysilane Si skeleton. The isolated skeleton pseudo- $\pi$ -band in polysilane is very different from that in polyethylene, where the skeleton pseudo- $\pi$ -band partly overlaps its own  $\sigma$ -like band.<sup>20</sup> This is consistent with the previous theoretical result that double bonds are not easily formed in chainlike polysilane skeleton.<sup>21</sup>

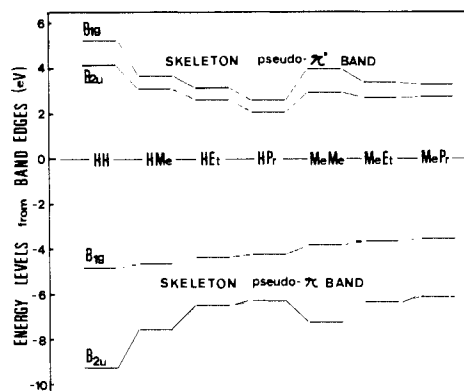


Figure 5. Skeleton pseudo- $\pi$ - and pseudo- $\pi^*$ -band energy levels of poly(alkylsilane). Symmetry assignment at the  $\Gamma$ -point is shown for  $(\text{SiH}_2)_n$  with  $D_{2h}$  symmetry.

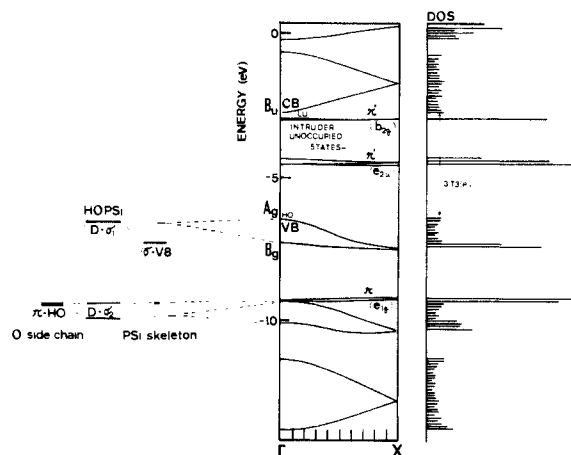


Figure 6. Energy band structure of  $(\text{SiHPh})_n$  model compound.  $\sigma$ - $\pi$  mixing between the polysilane (PSi) skeleton  $\sigma$ -VB state and the Ph side-chain  $\pi$ -HOMO levels is also illustrated.

**Polysilane Having Ph Side Chains: Poly(arylsilane).** The calculated band structure for poly(hydrophenylsilane),  $(\text{SiHPh})_n$ , is shown in Figure 6. The original skeleton band gap is 3.73 eV, and  $(\text{SiHPh})_n$  also yields a similar directly allowed type band structure. The CB bottom state is an antibonding one between skeleton Si-3s AOs with  $B_u$  symmetry, and the VB top is a bonding state between Si-3p AOs with some side-chain Ph  $\pi$ -HOMO characteristics. Both of these band-edge states are delocalized along the skeleton axis similar to other poly(organosilanes). The  $\sigma$ - $\sigma^*$  optical transition which corresponds to the skeleton band-to-band transition also occurs in  $(\text{SiHPh})_n$ .

The characteristic features of the  $(\text{SiHPh})_n$  electronic structure are a  $\sigma$ - $\pi$  band mixing at the VB edge state and an intrusion of six unoccupied localized levels in the original skeleton band gap. The poly(organosilane) skeleton VB edge is the  $\sigma$ -state which is formed by the bonding state between skeleton Si-3p<sub>x</sub> AOs and is well delocalized along the skeleton axis. Benzene HOMOs are doubly degenerated  $\pi$ -states whose orbital lobes are standing vertically with respect to the molecular plane. The energy difference between these two states is much less than the corresponding values between those of alkanes and benzene. Then, skeleton-side-chain interaction due to  $\pi$ -like coupling results in  $\sigma$ - $\pi$  band mixing between skeleton  $\sigma$ -VB (Si-3p<sub>x</sub>) and side-chain Ph  $\pi$ -HOMO (C-2p<sub>x</sub>) states. This  $\sigma$ - $\pi$  band mixing initially forms the following three occupied levels due to the double degeneracy of Ph  $\pi$ -HOMOs. The symmetric  $\pi$ -HOMO (corresponding to the benzene  ${}^{\text{sym}}e_{1g}$   $\pi$ -HOMO) is able to mix with the skeleton

(20) Karpfen, A. *J. Chem. Phys.* **1981**, *75*, 238.

(21) Dewar, M. J. S.; Lo, D. H.; Ramsden, C. A. *J. Am. Chem. Soc.* **1975**, *97*, 1311. For experimental synthesis of Si double-bonded oligomer, see: Masamune, S.; Hanazawa, Y.; Murakami, S.; Bally, T.; Blount, J. F. *J. Am. Chem. Soc.* **1982**, *104*, 1150.

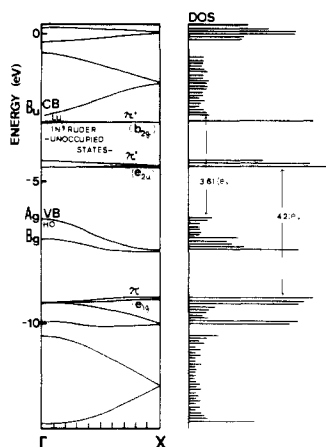


Figure 7. Energy band structure of  $(\text{SiMePh})_n$  model compound.

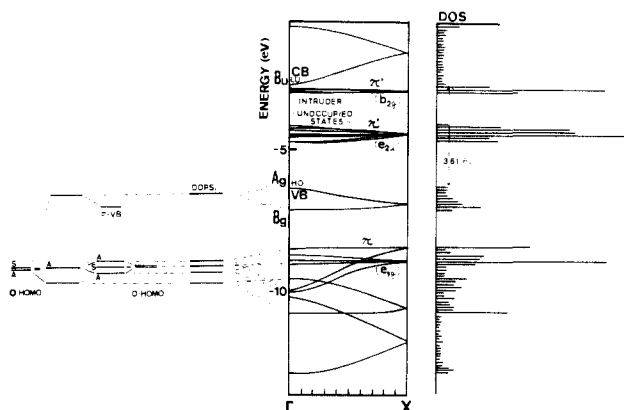


Figure 8. Energy band structure of  $(\text{SiPh}_2)_n$  model compound. Schematic  $\sigma$ - $\pi$  band mixing is also illustrated.

delocalized  $\sigma$ -VB. This results in the formation of two delocalized  $\sigma$ -states ( $D$ - $\sigma_1$  and  $D$ - $\sigma_2$ ). The asymmetry of the other  $\pi$ -HOMO (benzene  $^{asy}e_{1g}$   $\pi$ -HOMO) cancels this  $\sigma$ - $\pi$  mixing effect. The resulting state remains strongly localized in the individual Ph side chains, almost as if no  $\sigma$ - $\pi$  mixing had occurred at all.

The skeleton  $\sigma^*$ -CB is well delocalized along the skeleton axis. The Ph side chain has three unoccupied  $\pi^*$  states, which correspond to benzene  $e_{2u}$  (LUMO) and  $b_{2g}$ . However, the corresponding  $\sigma^*$ - $\pi^*$  band mixing does not take place in the CB bottom state. The reason is that the skeleton  $\sigma^*$ -CB state is formed of skeleton Si-3s AOs. This produces different magnetic quantum numbers between skeleton  $\sigma^*$ -CB and side-chain  $\pi^*$ -states, which inhibits the  $\sigma^*$ - $\pi^*$  band mixing. The resulting CB (excited) states retain the similar energy structure to that of poly(alkylsilane). This is why the unoccupied states which originate from the Ph side-chain group intrude independently in the skeleton band gap without band mixing.

A similar electronic structure can be obtained for poly(methylphenylsilane)  $-(\text{SiMePh})_n$  in Figure 7. The skeleton band gap is reduced to 3.61 eV ( $-(\text{SiMePh})_n$ ) by Me group substitution. The occupied level localized in the Me side chains is found in the lower energy state.

Figure 8 shows the resulting band structure of poly(diphenylsilane),  $-(\text{SiPh}_2)_n$ , whose side chains are fully substituted by Ph groups. The addition of one more Ph side-chain substituent produces a complicated band mixing as follows. The single skeleton-side-chain interaction in  $-(\text{SiMePh})_n$  produces two delocalized states and one localized state. This localized state in  $-(\text{SiPh}_2)_n$  is able to couple with the additional Ph  $\pi$ -HOMO (asymmetric) state. On the contrary, the remainder of the additional Ph  $\pi$ -HOMO (symmetric) states tend to remain localized in the individual Ph side chains rather than to mix with the two resulting delocalized states. Consequently, five resulting energy states are caused per one  $\text{SiPh}_2$  segment. This produces 10 band states in the polymer chain, because the unit cell has two  $\text{SiPh}_2$

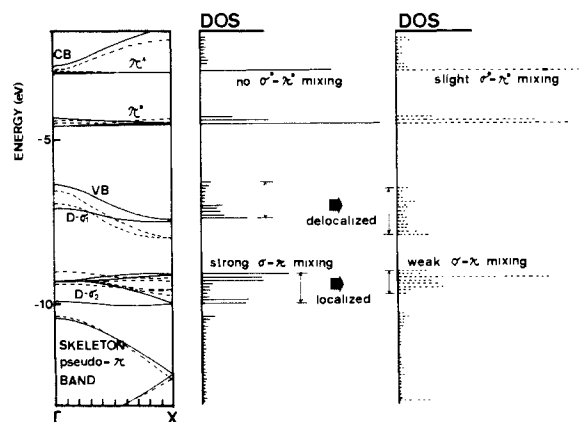


Figure 9. Electron localization-delocalization in mixed states by the rotation of the Ph side chain. Solid line means the resulting energy band structure and DOS of MePhPSi with a vertical dihedral angle between the skeleton plane and the Ph molecular plane. Broken lines on right indicate those for the resulting mixed state when the corresponding dihedral angle is changed to  $120^\circ$ .

segments. Ph  $\pi^*$ -LUMOs ( $e_{2u}$ ) are removed by the encounter of two Ph side-chain pendants, resulting in eight unoccupied states which intrude in the skeleton band gap. There are also four unoccupied intruders which originate from benzene  $\pi^*$  ( $b_{2g}$ ). An adjoining Ph side-chain arrangement enhances the  $\sigma$ -like interaction between these  $\pi^*$ -intruders through neighboring Ph side chains. This causes a slight delocalization of the intruders along the "skeleton direction" and produces weak dispersion.

This paper also considers how Ph side-chain rotation influences  $\sigma$ - $\pi$  or  $\sigma^*$ - $\pi^*$  band mixing at the corresponding band edges (Figure 9). The localization of the resulting states is sensitive to the Ph side-chain rotation, because that rotation affects the magnitude of the corresponding band mixing. Electrons in the slightly dispersed bands ( $D$ - $\sigma_2$ ) are most delocalized along the skeleton axis direction when Ph side chains are arranged to form a vertical dihedral angle between the Ph molecular plane and the skeleton plane. The reason is that this Ph side-chain arrangement produces the maximum  $\sigma$ - $\pi$  mixing at the VB-edge state. This arrangement also produces the most localized state for  $D$ - $\sigma_1$  electrons, since the localized Ph  $\pi$ -HOMO character is most effectively induced in the delocalized polysilane skeleton  $\sigma$ -VB state. The degree of  $\sigma$ - $\pi$  band mixing tends to decrease as the Ph side chains are rotated. On the contrary,  $\sigma^*$ - $\pi^*$  band mixing tends to increase as these side chains are rotated.  $\sigma^*$ - $\pi^*$  band mixing cannot occur when the dihedral angle of the skeleton side chain is arranged vertically. The rotation of the Ph side chain introduces a slight inclination in the Ph molecular plane (i.e., inclined Ph  $\pi$ -HOMOs). This inclination causes a weak  $\sigma^*$ - $\pi^*$  mixing between Si-3s AOs and C-2p AOs. This weak  $\sigma^*$ - $\pi^*$  mixing pulls the skeleton  $\sigma^*$ -CB edge down slightly. However, this has almost no influence on the intruders.

**Assignment of Experimental Photoabsorption Spectra.** Experimental photoabsorption spectra<sup>22</sup> for poly(organosilane) were assigned on the basis of the resulting band structure. The poly(organosilanes) used in the experiment were  $-(\text{SiMePr})_n$  and  $-(\text{SiMePh})_n$ . Both have a molecular weight of over  $10^4$ .

According to the band structure calculated for  $-(\text{SiMePr})_n$  (Figure 3), the absorption spectra originating from the  $\sigma$ - $\sigma^*$  interband optical transition is expected to appear at about 3.9 eV. This peak is also expected to be sharp because of the DOS divergence at the band edge due to poly(organosilane) one-dimensionality. A corresponding sharp absorption peak for  $-(\text{SiMePr})_n$  is found at 3.8 eV (Figure 10). This peak is, therefore, thought to reflect the  $\sigma$ - $\sigma^*$  interband transition.

According to the band structure calculated for  $-(\text{SiMePh})_n$  (Figure 7), the following optical transitions are expected. The lowest energy transition should be a  $\sigma$ - $\sigma^*$  transition through the original skeleton band gap. This peak is expected to be sharp and

(22) Fujino, M., private communication.

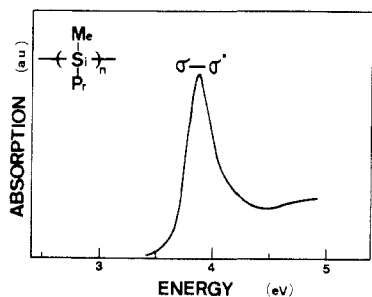


Figure 10. Experimental photoabsorption spectrum of  $(\text{SiMePr})_n$ .

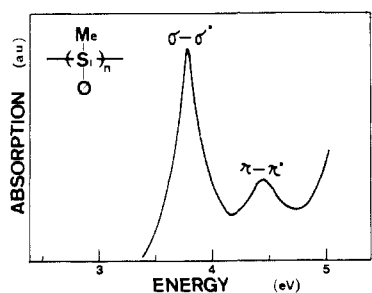


Figure 11. Experimental photoabsorption spectrum of  $(\text{SiMePh})_n$ .

also to appear in a similar energy region (3.7 eV) slightly less than that of  $(\text{SiMePr})_n$ . The next possible transition is a  $\pi-\pi^*$  transition, which occurs in the individual Ph side chains and corresponds to the benzene  $\pi-\pi^*$  transition.

Two characteristic absorption peaks are observed for  $(\text{SiMePh})_n$  (Figure 11). The sharp of the peak at 3.7 eV is similar to that in  $(\text{SiMePr})_n$ . The other peak is observed at about 4.5 eV, which is inherent in  $(\text{SiMePh})_n$ . The experimental photoabsorption spectra can thus be assigned as follows. The peak at 3.7 eV is thought to originate from the  $\sigma-\sigma^*$  interband transition

on the skeleton axis. The peak at 4.5 eV corresponds to the  $\pi-\pi^*$  transition in the Ph side chains.

### Summary

Poly(organosilane) exhibits a directly allowed type band structure. The existence of the isolated skeleton  $\pi$ - and  $\pi^*$ -like bands causes the skeleton  $\sigma$ - and  $\sigma^*$ -band-edge states to be displaced upwards. This feature is significantly different from the corresponding electronic structure of polyethylene. The poly(organosilane) band-edge states are formed mainly of skeleton Si AOs, which produces the skeleton band gap. This skeleton band gap tends to be compressed when larger alkyl groups are substituted in side chains. The amount of reduction is not significant, however, because of the weak electronic contribution from the side chains.

In poly(arylsilane), the  $\sigma-\pi$  band mixing due to skeleton-side-chain interaction changes the poly(alkylsilane) single VB structure to a multiple structure. Two of them are delocalized along the skeleton axis, and the other is localized in the individual Ph side chains. On the contrary, no  $\sigma^*-\pi^*$  band mixing occurs in the CB states, and no change is seen in the CB structure. The unoccupied  $\pi^*$ -states localized in the individual Ph side chains also intrude in the skeleton band gap.

The well-delocalized band-edge states seen in polysilane suggest that simple band conduction occurs along the skeleton Si axis for both electrons and holes. When Ph groups are used as the side chains (poly(arylsilane)), electrons and/or holes are localized in Ph side chains as well as delocalized along the skeleton axis. For these materials, carries in localized  $\pi$ - and/or  $\pi^*$ -states tend to exhibit hopping conduction between Ph side chains, in addition to the band conduction by carriers in the delocalized skeleton band-edge states.

**Acknowledgment.** We would like to express thanks to Dr. M. Fujino for contributing the experimental photoabsorption data used in this work. Thanks are also due to Dr. K. Sugii for his helpful discussions.

## $^{13}\text{C}$ Differential Line Broadening and the Experimental Measurement of the Absolute Signs of the One-Bond Carbon-Hydrogen Spin-Coupling Constants in Phenylacetylene<sup>†</sup>

Thomas C. Farrar,\* Bruce R. Adams, Gothard C. Grey, Rafael A. Quintero-Arcaya, and Qihui Zuo

Contribution from the Department of Chemistry, University of Wisconsin, Madison, Wisconsin 53706. Received May 7, 1986

**Abstract:** The widths of the carbon-13 resonance lines in phenylacetylene have been measured as a function of temperature and magnetic field strength. The line widths of the various carbon-13 doublets are differentially broadened due to interference effects caused by the presence of two relaxation mechanisms, dipolar and chemical shift anisotropy, which have common correlation times. Since the signs of the chemical shift anisotropies for the acetylenic and aromatic carbons are known from independent solid-state measurements, the absolute sign of the carbon-hydrogen spin-coupling constant can be determined from the differential line broadening. For the acetylenic carbon  $J_{\text{C-H}} = +252.1$  Hz at  $-30$  °C. For the ring carbon para to the acetylene, which lies on the symmetry axis,  $J_{\text{C-H}} = +162.1$  Hz.

During the past year or so reports have been given of differential line broadening (DLB) in simple two-spin systems such as  $^{31}\text{P}-\text{H}^1$  and  $^{13}\text{C}-\text{H}^2$ . No clear explanation of the effect was given in the

reports. We have shown<sup>3</sup> that the observed differential transverse relaxation (which determines the observed NMR line widths) is

(1) Lunsford, J. H.; Rothwell, W. P.; Shen, W. *J. Am. Chem. Soc.* **1985**, *107*, 1540.

(2) Macura, S.; Brown, L. R. *J. Magn. Reson.* **1985**, *62*, 328.

<sup>†</sup>A brief summary of this work was presented at the 27th ENC Meeting, April 16, 1986, in Baltimore, MD.